

Numerical Analysis and Measurement of Non-Uniform Torsion

J. Murin¹, T. Sedlar¹, V. Kralovic¹, V. Goga¹, A. Kalas¹ and M. Aminbaghai²

¹Department of Applied Mechanics and Mechatronics UEA
Faculty of Electrical Engineering and Information Technology
Slovak University of Technology in Bratislava, Slovakia

²Institute for Mechanics of Materials and Structures
Vienna University of Technology, Austria

Abstract

The subject of the present paper is an innovative approach to the investigation of the non-uniform torsional behaviour of prismatic beams taking into account the secondary torsional moment deformation effects. This investigation contains computational and experimental parts for both open and closed thin-walled cross-sections. Results of original experimental measurements of some warping-torsion features will be presented and compared with the ones obtained analytically and numerically. The necessity of considering the warping effects for closed thin-walled beams are studied and evaluated. The accuracy and the correctness of the results obtained are evaluated and discussed. The main novelty in this study is the measurement of some of the most important warping parameters, especially for closed cross-sections. These measurements prove the importance of warping consideration in non-uniform torsion of open and closed thin-walled profiles, and also the necessity of considering the secondary torsion moment deformation effect, especially in closed cross-sections.

Keywords: non-uniform torsion, warping, open and closed cross-sections, measurement and numerical calculation, secondary torsional moment deformation effect.

1 Introduction

The effect of warping must be assumed in stress and deformation analyses of structures above all with thin-walled cross-sections loaded by torsion. Warping effects occur mainly at the points of action of the concentrated torsion moments (except for free beam ends) and at sections with free-warping restrictions. Special theories of torsion with warping – non-uniform torsion – have been used to solve such problems analytically (e.g. [1]). The analogy between the 2nd order beam theory (with tensional axial force) and torsion with warping is also very often used

(e.g. [2], [3]). One has to point out that in the literature and practice, as well as in the EC-3 [4] and EC-9 [5] guidelines, strong warping is assumed to occur in open cross-sections only. Warping-based stresses and deformations in closed sections, however, are assumed to be insignificant and have been therefore neglected.

According to the above mentioned theory of torsion with warping and the analogy, special 3D-beam finite elements have been designed and implemented into the finite element codes (e.g. [6], [7]). The warping effect is included through an additional degree of freedom at each nodal point - the first derivative of the angle of twisting of the beam cross-section. Important progress in the solution of torsion with warping has been reached in papers [8] and [9] where a combination of boundary and finite element method was used allowing a warping analysis for composite beams with longitudinally varying cross-section.

However, latest theoretical results have shown that the effect of warping must be considered in the case of non-uniform torsion of closed-section beams [10]. For prismatic beams, the analogy between the torsion with warping (including the secondary torsion moment deformation effect) and the 2nd order beam theory (including the shear force deformation effect) has to be used. This approach was implemented into the computer code IQ-100 [13]. This analogy does not hold for non-prismatic beams [11]. According to the last research results in this area ([10], [11], [12], [14]), the local stiffness relation of a new two-node finite element for torsion with warping of straight beam structures is presented in contribution [15]; again based on the above-mentioned analogy. The warping part of the first derivative of the twist angle has been considered as the additional degree of freedom in each node at the element ends which can be regarded as part of the twist angle curvature caused by the warping moment. This new finite element can be used in non-uniform torsion analyses of constant open and closed cross-section beams. Finally in [16], the boundary element method has been applied in the non-uniform torsion analysis of simply or multiply connected bars of doubly symmetrical arbitrary constant cross-section, taking into account secondary torsional moment deformation effects. Necessity of the non-uniform torsion effect in the analysis of close shaped cross-section has been confirmed.

It has been concluded in various papers and studies (e.g. [11], [15], [16]) that results given by the classical thin tube theory and numerical analyses can differ significantly in the stress calculation especially in the analysis of the closed cross-sections if the effect of secondary torsion moment deformation effect is neglected. Additionally, the inaccuracy of the thin tube theory in calculating the secondary torsion constant even for closed thin-walled cross-sections has been observed in [16], [17].

Hence, it is straightforward to carry out measurements of the most significant features of non-uniform torsion: the total torsion angle, warping displacement and the normal stress caused by bimoment. The measurement results can then be used in evaluation of the calculated results obtained by several theories and commercial software outputs. It is worth here noting that there is a lack of relevant experimental results available in literature. This was a strong motivation for the authors to deal with design of a new measurement device which would be able to measure some deformation effects and normal stress caused by non-uniform torsion. The aim of

this paper is also the presentation of this new measurement device [18] which was used in verification and evaluation of the results obtained by the above mentioned theories. Predominantly, the measurement of some major warping effects will bring proof for the necessity of normal (bimoment) stress consideration in the design and analysis of closed thin-walled beams.

2 Design of the measurement device

The measurement device (Figure 1) consists of a welded base frame to which the measured beam is attached via a set of supporting clamps enabling fixed (clamped) binding. At this particular position, all six DOFs are restrained. Four closed-section braces are welded onto the base holding a circular bearing jewel in which a radial ball-bearing is set. A hollow two-arm-hub is rotating in the bearing. Dimensions of the measured beam are limited by the hole of the hub. An exchangeable steel hub-disc is designed to enable torsion moment application – via a twisting force couple – onto individual beams. The force application is realized by two teflon screws with spherical endings. The hub-disc is fastened to the hub via four safety bolts. The centre-line of the hub's arms runs through the centre of the measured sample. Both arms have specially shaped cut-offs with splineways and holes. The tension wires are guided through splineways, set of rollers to a tension gear. This mechanism enables the torque application and restrictions at one end of the beam result in non-uniform torsion. The measurement device provides opportunities to measure some parameters of non-uniform torsion. A laser-device is fixed on one of the rotating hub-arms while its projection (e.g. onto a wall) enables the total torsion angle calculation. The total warping displacements is measured via a micro-displacement-meter. Longitudinal normal (bimoment) stress distribution is calculated from measured values of strain via a set of attached resistant strain gauges and a logger. Results are then compared with theoretical predictions.

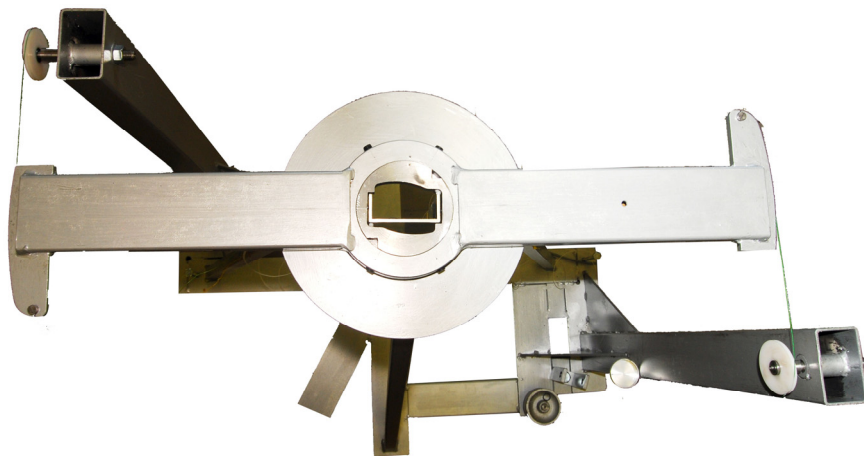


Figure 1: Prototype of the measurement device – the mechanical parts.

Mechatronic set-up (Figure 2) used for the measurement of non-uniform torsion deformation and stress is as follows: linear strain gauges (HBM 6/12LY11 type), universal amplifier QuantumX MX440 A and a laptop with software for acquisition of measurement data Catman®Easy.



Figure 2: The measurement parts and equipments.

The measurement device was designed and fabricated at Department of Applied Mechanics and Mechatronics of IEAE of FEI STU in Bratislava.

3 Theoretical base for torsion with warping including the secondary torsion moment deformation effect

3.1 Semi-analytical approach

As previously mentioned, the effect of warping must be considered also in the case of torsion of constant closed-shaped cross-sections [3], [11], [14]. The analogy between the torsion with warping (including the secondary torsion moment deformation effect) and the 2nd order beam theory with tensional axial force (including the shear force deformation effect) can be used in this case. The analogical variables and constants, differential expressions and equations, boundary conditions and expressions for stress and deformations calculations are described in [14] in full length.

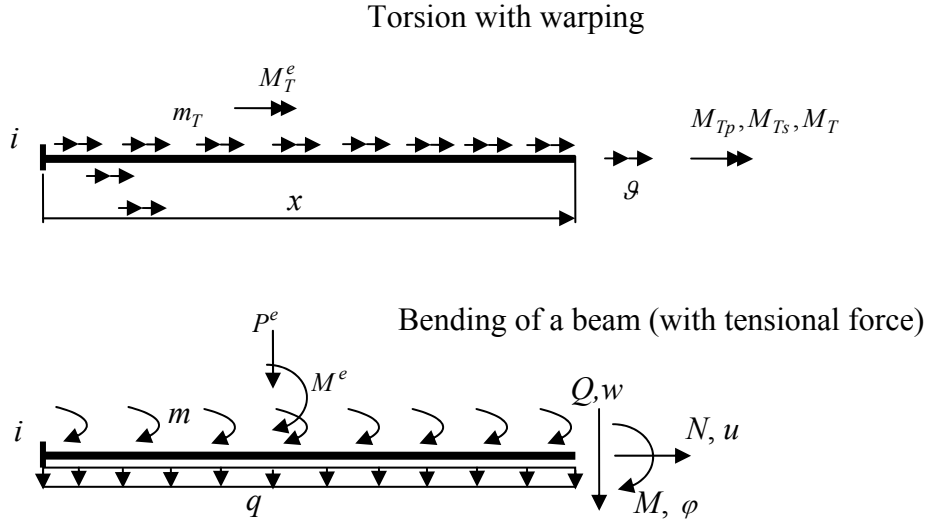


Fig. 3. Analogical state variables

Similar to the derivation of transfer matrices for the 2nd order beam theory for constant cross-section under shear force deformation effect, and after implementation of the analogical variables according to Figure 3, the transfer matrix for torsion with warping has been constructed [3]:

$$\begin{bmatrix} \mathcal{G} \\ \mathcal{G}' \\ M_M \\ M_\omega \\ M_{Ts} \end{bmatrix} = \begin{bmatrix} 1 & a_1 & -\kappa k_2 & -k_3 \\ 0 & 1 & -k_1 & -k_2 \\ 0 & 0 & b_0 & b_1 \\ 0 & 0 & Kb_1 & b_0 \end{bmatrix} \cdot \begin{bmatrix} \mathcal{G}_i \\ \mathcal{G}'_{Mi} \\ M_{\omega i} \\ M_{Tsi} \end{bmatrix} \quad (1)$$

with $K = \kappa \frac{GI_T}{EI_\omega}$ and $f = \sqrt{K}$ being the transfer functions b_j derived as:

$$b_0 = \cosh(fx), \quad b_1 = \frac{\sinh(fx)}{f}, \quad \text{for } j \geq 2: b_j = \frac{b_{j-2} - a_{j-2}}{K}$$

and with $a_0 = 1$, for $j \geq 1: a_j = \frac{x^j}{j!}$.

These transfer functions can be calculated also by the special exponential functions described in [10]. Here: $\mathcal{G} = \mathcal{G}(x)$ - is the twist angle transfer function and \mathcal{G}_i is its value at node i ; $\mathcal{G}'_M = \mathcal{G}'_M(x)$ - is the warping part of the first derivative of the twist angle transfer function and \mathcal{G}'_{Mi} is its value at node i ; $M_\omega = M_\omega(x)$ - is the bimoment transfer function and $M_{\omega i}$ is its value at node i ; $M_{Ts} = M_{Ts}(x)$ is the

secondary torsion moment transfer function and M_{Tsi} is its value at node i . The

$$\text{stiffness constants are: } k_1 = \frac{b_1}{EI_\omega}; k_2 = \frac{b_2}{EI_\omega}; k_3 = \left(\frac{b_3}{EI_\omega} - \frac{b_1}{GI_{Ts}} \right).$$

The arbitrary cross-sectional characteristics are described by: A – cross-sectional area [m²]; I_T – torsion constant [m⁴]; I_{Ts} – secondary torsion constant [m⁴]; I_ω – warping constant [m⁶]. Material properties: E – elasticity modulus; G – shear modulus.

The secondary torsion moment deformation effect is encountered through constant

$$\kappa = \left(1 + \frac{I_T}{I_{Ts}} \right) \text{ and the transfer constants } b_j, j \in \langle 0,3 \rangle. \text{ Parameter } \kappa = 1 \text{ if this effect is}$$

neglected. This is usually made in the case of open form cross-sections where the effect of the secondary torsion moment has been assumed insignificant. Deformation effect of the secondary torsion moment must be considered first of all in the case of the closed form cross-sections as demonstrated in [3].

The expressions for calculation of the secondary torsion constant (denoted as I_{Ts}) depend on the cross-section type. These can be found in [8] and [12], for example.

This approach was implemented into the computer code IQ-100 [13], which can be used in analysis of torsion with warping of the closed and opened thin walled cross-sections.

3.2 Finite and boundary element method approach

The above-described transfer functions with $x = L$ (L is the length of the rod) have been originally used to establish the local stiffness relation of the finite element for torsion of a straight beam structure with warping [15]. Despite authors' efforts, no other finite element designed for warping-torsion including the secondary torsion deformation effect has been found in literature to the present date.

Significant contribution, from point of view of secondary torsion moment consideration and verification of necessity of the warping inclusion into the torsion of the solid and closed cross section analysis, was presented in papers [16] and [17]. In these papers, the Boundary Element Method (BEM) has been used for the solution of such problems inclusive calculation of the secondary torsion and warping constants.

Figure 4 shows a prismatic beam element of length L with two nodes i and k , and with appropriated geometric, static, kinematics and material quantities as described above by the semi-analytical approach. In comparison with Figure 3, the classical finite element method definition has been used for positive orientation of the nodal variables for this approach.

In order to include the warping, a new degree of freedom is added to the classical nodal variables in the stiffness matrix in each element nodal point. The warping part of the first derivative of the twist angle (\mathcal{G}'_M) has been originally considered as the additional degree of freedom in each node at the element ends. This can be regarded as part of the twist angle curvature which is caused by the warping moment.

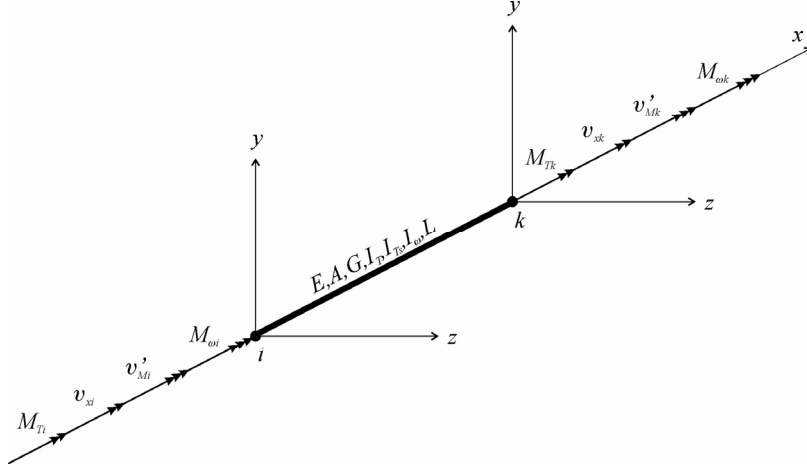


Figure 4: Prismatic finite element for torsion.

This choice brings advantages when applying the boundary conditions. If the secondary torsion moment deformation effect is not considered $\mathcal{G}'_M(x) = \mathcal{G}'(x)$. The nodal displacement vector in the local coordinate system, as shown in Fig. 4, is

$$\{u^e\}^T = \{\mathcal{G}_i \quad \mathcal{G}'_{Mi} \quad \mathcal{G}_k \quad \mathcal{G}'_{Mk}\} \quad (2)$$

and the respective nodal load vector is

$$\{F^e\}^T = \{M_{Ti} \quad M_{oi} \quad M_{Tk} \quad M_{ok}\} \quad (3)$$

where M_{Ti} and M_{Tk} are the torsion moments, M_{oi} and M_{ok} are the warping moments at the nodal points. The geometrical meaning of all these kinematics and static variables is evident from Figure 4.

Using the aforementioned transfer matrix relations (1) (after some mathematical manipulations) the element local stiffness relation for torsion with warping (including the secondary torsion moment deformation effect) has been derived. The resultant relation can be written as [15]:

$$\begin{Bmatrix} M_{Ti} \\ M_{oi} \\ M_{Tk} \\ M_{ok} \end{Bmatrix} = \frac{k_2}{\kappa k_2^2 - k_1 k_3} \cdot \begin{bmatrix} \frac{k_1}{\kappa k_2} & -1 & -\frac{k_1}{\kappa k_2} & -1 \\ -1 & \left(\kappa b_1 - b_0 \frac{k_3}{k_2} \right) & 1 & \frac{k_3}{k_2} \\ -\frac{k_1}{\kappa k_2} & 1 & \frac{k_1}{\kappa k_2} & 1 \\ -1 & \frac{k_3}{k_2} & 1 & \left(\kappa b_1 - b_0 \frac{k_3}{k_2} \right) \end{bmatrix} \cdot \begin{Bmatrix} \mathcal{G}_i \\ \mathcal{G}'_{Mi} \\ \mathcal{G}_k \\ \mathcal{G}'_{Mk} \end{Bmatrix} \quad (4)$$

For the straight beam structures the local relation (4) coincides with the global one. The implementation of the expression (4) into the local equation of the 3D-beam finite element is straightforward, and it will be done in our future work.

When the kinematic and static variables in (4) are known at the nodal points, the primary and secondary torsion moment, normal and shear stress can be calculated in a usual way [19]. The nodal points' secondary torsion moments are:

$$M_{Tsi} = \kappa(M_{Ti} - GI_T \mathcal{G}'_{Mi}); \quad M_{Tsk} = \kappa(M_{Tk} - GI_T \mathcal{G}'_{Mk}) \quad (5)$$

The primary torsion moments at the nodal points are:

$$M_{Tpi} = M_{Ti} - M_{Tsi}; \quad M_{Tpk} = M_{Tk} - M_{Tsk} \quad (6)$$

Expressions for the shear and normal stress calculation depend on the cross-sectional area type. This problem has been described in detail in [10]. These expressions will be now used for stress calculations in our numerical examples. This new finite element can be used for analysis of torsion with warping of constant both open and closed-shaped cross-sections.

4 Numerical experiment and measurement of non-uniform torsion of cantilever beams

The aim of this chapter is the experimental verification of theoretical findings that the analogy between the torsion with warping (including the secondary torsion moment deformation effect) and the 2nd order beam theory with tensional axial force (including the shear force deformation effect) holds. The most important verification is the experimental proof of the necessity of warping consideration in closed thin-walled cross-sections loaded by torsion. Torsion of clamped prismatic beams of both open and closed cross-sections will be studied. Obtained results will be evaluated and discussed.

4.1 U-beam loaded by torsion with warping

The aim of the following investigation is the measurement and calculation of the total twisting angle, total warping displacement at the unrestrained end of the beam. The normal stress flow along the web of the U-beam caused by the bimoment will be determined.

A prismatic cantilever aluminium beam of length $L = 0.821$ m and constant U-shaped cross-section ($E = 79$ GPa – Young modulus, $G = E/(2(1+\nu)) = 31.1$ GPa – shear modulus, $\nu = 0.27$ - Poisson ratio), loaded by torsion moment $M = 5.29$ kNm at its free end is depicted in Fig. 5.

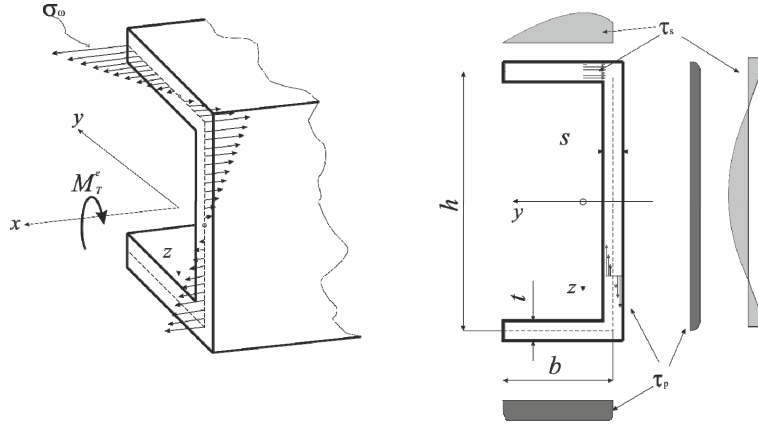


Figure 5: Geometrical parameters, normal and shear stress distribution.

According Figure 5, the following cross-section parameters have been chosen and calculated [12], [19]: $h = 0.07$ m, $b = 0.0285$ m, $t = s = 0.003$ m, $A = A_s + 2A_G = hs + 2bt = 0.000381$ m² – the cross-sectional area containing the area of the web A_s and the area of flange plates A_G , $\bar{e} = \frac{3}{6 + A_s / A_G} = 0.3547717842$ – the auxiliary constant,

$e = \frac{b}{2 + \frac{A_s}{3A_G}} = 0.011828883$ m – the eccentricity of the shear centre, $\omega_1 = eh/2 =$

$= 0.00041401092$ m², $\omega_2 = (b - e)h/2 = 0.000583489077$ m² – warping ordinate at corners 1 and 2, $I_\omega = (\omega_1^2 + \omega_2^2 - \omega_1\omega_2) \frac{2A_G}{3} + \omega_1^2 \frac{A_s}{3} = 2.653384408 \times 10^{-11}$ m⁶ – the

warping constant; $I_T = \frac{1}{3}(2A_G t^2 + A_s s^2) = 1.656 \times 10^{-9}$ m⁴ – the torsion constant,

$S_1 = \frac{b - e}{b} A_G \frac{\omega_2}{2} = 1.775316237 \times 10^{-8}$ m⁴, $S_0 = S_1 \left(1 - \left(\frac{e}{b - e} \right)^2 \right) = 1.238596992$ m⁴,

$\alpha = 1 - 2\bar{e} = 0.2904564316$ and $\beta = \frac{2}{3} - \bar{e} = 0.3118948825$ – auxiliary constants,

$I_{Ts} = \frac{(\beta b h)^2}{\left(2\beta^2 + \frac{\alpha^2}{6} + \frac{1}{90} \right) \frac{b}{t} + \frac{\alpha^2 h}{5s}} = 1.560462784 \times 10^{-7}$ m⁴ – the secondary torsion

constant. Parameters S_1 and S_0 are used in shear stress calculation.

The beam was analyzed with program ANSYS [6], IQ-100 [13], and with new effective beam element [15].

Prior to the clamping and setting of the beam within the measurement device, a set of linear gauges needs to be glued onto the beam surface. At this point, one has to point out that the normal stress (and strain) is a function of all coordinates, i.e. bimoment changes with the longitudinal direction and warping ordinate changes

along the camber line. Therefore a special care has to be given to this process. In our experiment, six linear strain gauges ($T_1 - T_6$) are glued to the tension side of the aluminium beam along its length (Figure 6). Three of them have (T_1 , T_2 and T_5) have a pair gauge (T_7 , T_8 and T_9) placed exactly on the opposite (compression) side of the beam as a mirror image. The correct set-up is affirmed when each pair of gauges shows identical absolute values of stress.

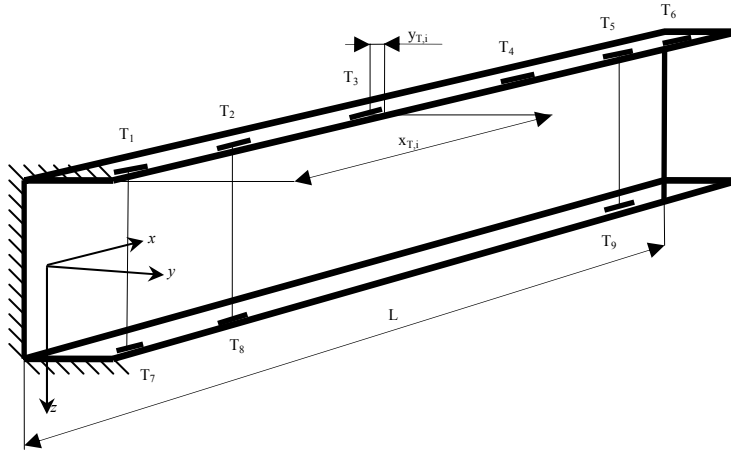


Figure 6: Positioning of the strain gauges.

The twisting force couple (torque) was applied via insertion of weights to the tension mechanism of the measurement device. Four values of twisting angle were generated and each measurement was repeated ten times. Average values were then used for the comparison with theoretical results.

In theoretical analysis, the outputs being the bimoment, primary and secondary torsional moment. These values were determined using the software IQ-100. Normal and shear stresses (Figure 5) at any point of the beam can be calculated according to [1], [12], [13] and [18], respectively. For this particular U-beam the calculated parameters are as follows: maximal normal stress $\sigma_\omega = 31.22$ MPa, maximal primary shear stress $\tau_{p,f} = 13.04$ MPa in the flange, maximal secondary shear stress $\tau_{s,w} = 1.18$ MPa in the middle of the web. The total torsion angle is $\varphi = 5.96^\circ$.

Maximum warping displacement calculated is $x_\omega = \int_{(l)} \frac{\sigma(x)}{E} dx = 210 \mu\text{m}$.

The numerical calculations were obtained using the Beam188 element specially designed within the ANSYS software [6]. A fine mesh was used in order to acquire the bimoment flow as well as normal and shear stress distribution. Geometrical and warping parameters are identical with the ones calculated analytically (see above) hence the normal stress $\sigma_{\omega,AN}$ flow will be derived from ANSYS' bimoment output.

Maximum normal stress is $\sigma_{\omega,AN} = 30.99$ MPa. The inputs for shear stress calculation, e.g. the primary and secondary torsion moments are not available, i.e. only a summation of primary and secondary shear stresses is generated for each

element. Therefore, at this stage, the experimental analysis will also be restrained to normal stresses only.

The measured sample (Figure 6) has been set within the measurement device according to the process described in the measurement set-up section above. The applied twisting force couple generating a torque of $M_T^e = 5.29$ kNm and the restrictions at the clamped end result in its non-uniform torsion (and bimoment distribution). The measurement of normal stress flow along the beam's length has been carried out at six positions (Figure 6). Due to the nature and size of the linear gauges it is impossible to position them at the very end of the camber line. Their positions can be estimated with the precision of about 0.25 mm and need to be taken into account when used in comparisons with other methods. Gauges' positions ($x_{T,i}$ - longitudinal, $y_{T,i}$ - distance from camber end), measured normal stress $\sigma_{\omega,ex}$, analytical calculations - $\sigma_{\omega,an}$ (in accordance with [1], [3], [13], [15], respectively) and FEM calculations with ANSYS - $\sigma_{\omega,FEM}$, as well as the difference evaluations $\delta_{ex/an}$ are present in Tab. 1.

analyzed position			normal stress			difference
gauge	$x_{T,i}$ [mm]	$y_{T,i}$ [mm]	$\sigma_{\omega,ex}$ [MPa]	$\sigma_{\omega,an}$ [MPa]	$\sigma_{\omega,FEM}$ [MPa]	$\delta_{ex/an}$ [%]
T ₁ / T ₇	10	4	22.45	23.32	25.11	3.7
T ₂ / T ₈	95	4.5	16.09	16.31	17.02	1.4
T ₃	200	2.75	12.88	11.65	11.72	10.5
T ₄	400	2.75	5.92	5.02	4.98	18
T ₅ / T ₉	650	2.75	2.78	1.36	1.38	104
T ₆	750	2.5	1.83	0.53	0.54	247.2

Table 1: Comparison of calculated and measured normal stresses in beam's longitudinal direction.

The difference value is calculated as: $\delta_{ex/an} = 100 \cdot |(\sigma_{\omega,an} - \sigma_{\omega,ex}) / \sigma_{\omega,an}|$. The first four measurements are in good agreement with the theory and numerical results. For the last two, the total difference is of about 1.5 MPa. This can refer to the well-known fact that for small strains linear gauges do not give accurate results. The total torsion angle measured is $\varphi = 6.12^\circ$ and the maximum warping displacement $x_\omega = 197$ μm . Both agree well with analytical and numerical predictions.

A more visual interpretation of the normal stress flow is in Figure 7. Theoretical and numerical results do not show any significant difference among themselves.

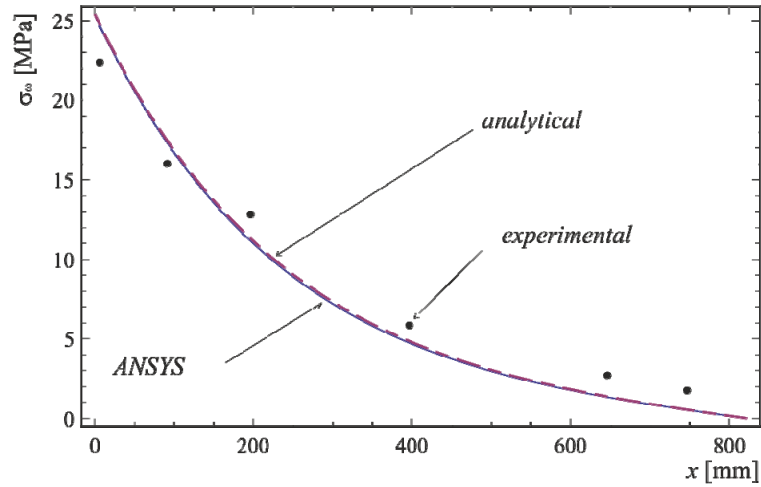


Figure 7: Normal stress flow along the beam length: measured values in comparison with numerical (ANSYS Beam188) and analytical results at gauges' positions.

4.2 Closed-section beam loaded by non-uniform torsion

As discussed earlier, in literature and papers there is a lack of available experimental evidence of non-uniform torsion behaviour for closed-section beams. In this sub-chapter, the authors present a complex analytical, numerical and experimental study of a closed-section prismatic beam loaded by non-uniform torsion bringing an experimental proof of the necessity of warping consideration for such structures. In addition, a large disproportion in calculations of torsion and warping constants using various analytical and numerical approaches will be shown and discussed.

In the analysis, measurements and calculations for the total twisting angle, the total warping displacement at the unrestrained end and normal stress flow will be discussed. The measured material properties of the prismatic cantilever aluminium beam (Figure 8) are as follows: Young modulus $E = 79$ GPa, shear modulus $G = E/(2(1+\nu)) = 31.1$ GPa and Poisson ration $\nu = 0.27$.

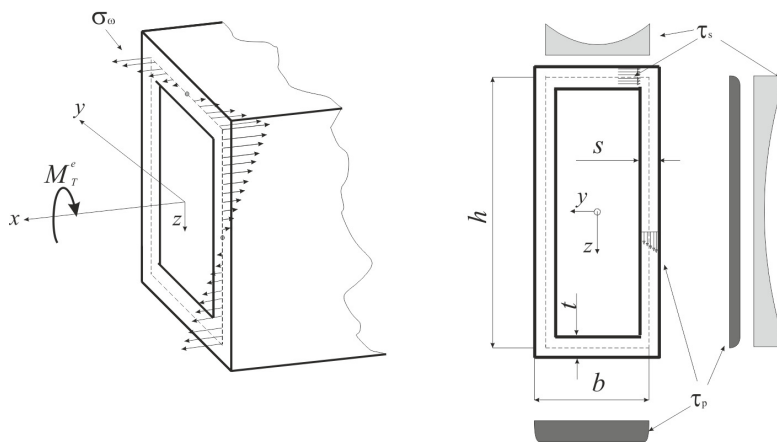


Figure 8: Geometrical parameters, normal and shear stress distribution.

According Figures 8 and 9, the following geometrical parameters have been chosen and calculated [12], [19]: $L_1 = 0.8$ m, $L_2 = 0.15$ m, $h = 0.058$ m, $b = 0.018$ m, $t = s = 0.002$ m, $A = 2A_s + 2A_G = 2(hs + bt) = 0.000304$ m² - the cross-sectional area containing the area of the webs A_s and flanges A_G , $\omega_R = \frac{hb}{4} \frac{ht - bs}{ht + bs} = 137.368 \times 10^{-6}$ m² - warping ordinate at the corners, $I_\omega = \omega_R^2 \frac{2A}{3} = 1.91217 \times 10^{-12}$ m⁶ - the warping constant; $I_T = \frac{2(hb)^2}{h/s + b/t} = 5.73651 \times 10^{-8}$ m⁴ - the torsion constant, $I_{Ts} = \frac{20(h/s + b/t)I_\omega A}{\frac{(Ahb)^2}{A_s A_G} + \frac{2(h^2 + b^2)^2}{3}} = 1.4589 \times 10^{-8}$ m⁴ - the secondary

torsion constant.

The beam was analyzed using the ANSYS [6] and IQ-100 [13] software, respectively and with new effective beam element [15].

The clamping process has been followed exactly as in section 4.1. In our analysis, five linear strain gauges ($T_1 - T_5$) are glued to the tension side of the aluminium beam along its length (Figure 9). Gauge T_1 has a pair gauge T_6 placed exactly on the opposite (compression) side of the beam as a mirror image. The correct set-up is affirmed when the pair shows identical absolute values.

The twisting force couple (torque) generating a torque of $M_T^e = 100$ Nm was applied via the tension-wire mechanism of the measurement device at position L_1 . In combination with restrictions at the clamped end and position of the torque, this set-up resulted in non-uniform torsion and bimoment distribution (Figure 10). Four values of twisting angle were generated and each measurement was repeated ten times. Average values were then used for the comparison with theoretical results.

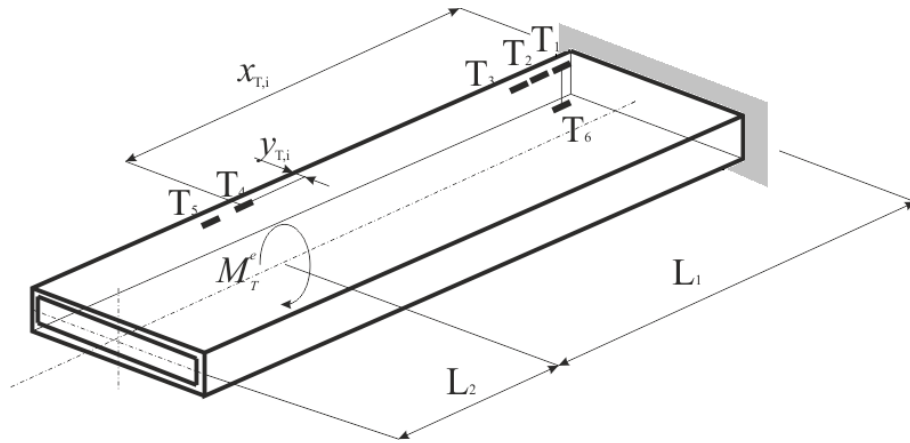


Figure 9: Positioning of the strain gauges.

In theoretical analysis, the outputs being the bimoment, primary and secondary torsional moment. These values were determined using the classical TTT [1] and the software IQ-100. Normal and shear stresses (Fig. 8) at any point of the beam can be calculated according to [1], [12], [13] and [18], respectively. For this particular

beam and the torsion moment $M_T^e = 100$ Nm, the calculated parameters are as follows: maximal bimoment $M_\omega = 0.41$ Nm², normal stress $\sigma_{\omega,an} = \frac{M_\omega \omega_R}{I_\omega} = 29.77$ MPa, maximal primary shear stress $\tau_{p,max} = \frac{M_{Tp}}{2hbt} = 23.95$ MPa, maximal secondary shear stress $\tau_{s,max} = \frac{M_{Ts}}{I_\omega t} \cdot \frac{\omega_R}{\frac{A_G}{4} + \frac{h^2 + b^2}{6(h/s + b/t)}} = 16.27$ MPa. The total torsion angle is $\varphi = 2.56^\circ$. Maximum warping displacement calculated is $x_\omega = \int_{(l)} \frac{\sigma(x)}{E} dx = 0.185$ μm ; this value is strongly influenced by the torque position and bimoment distribution.

The numerical calculations were also obtained using the ANSYS' Beam188 element [6]. A fine mesh was used in order to acquire the bimoment flow as well as normal and shear stress distribution. Warping parameters, in particular the warping constant $I_{\omega,FEM} = 2.15 \times 10^{-12}$ m⁶, differ from analytical calculations (as pointed out in e.g. [16], [17]). Moreover, the element table output data for bimoment at the clamped end give $M_{\omega,FEM} = 0.81$ Nm² and the corresponding maximum normal $\sigma_{\omega,FEM} = 63.41$ MPa - twice the value determined analytically [1] and [3]. The inputs for shear stress calculation are not available (see section 4.1).

Comparison of analytical and numerical calculations of the cross-sectional and warping parameters, maximum bimoment and normal stress values are presented in Table 2. The bimoment flow is depicted in Figure 10.

<i>parameter</i>	ANSYS Beam188	TTT Rubin	TTT classical
I_T [mm ⁴]	59042	57365	57365
I_{TS} [mm ⁴]	-	14589	-
I_ω [mm ⁶]	2150000	1912168	1912170
ω_R [mm ²]	-	137.37	137.37
M_ω [Nm ²]	0.81	0.41	0.48
σ_{max} [MPa]	63.41	29.77	34.79

Table 2: Cross-sectional and warping parameters, maximum bimoment and normal stress comparisons: numerical and analytical calculations.

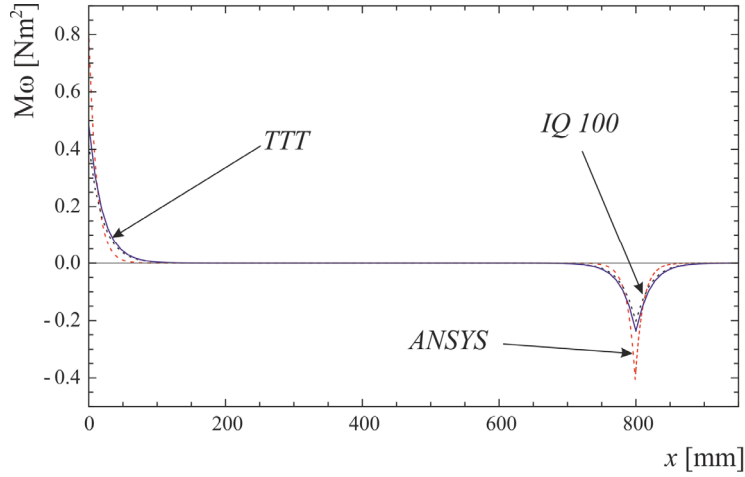


Figure 10: Bimoment flow: FEM calculation obtained via ANSYS Beam188, classical TTT [1] and semi-analytically [3],[13].

The measurement of normal stress flow along the beam's length has been carried out at 5 positions; gauges positions $x_{T,i}$ and $y_{T,i}$ (Figure 9), corresponding measured normal stress $\sigma_{\omega,ex}$, analytical calculations $\sigma_{\omega,an}$ [3] and FEM calculations with ANSYS Beam188 $\sigma_{\omega,FEM}$ as well as the difference evaluations $\delta_{ex/an}$ are present in Table 3. The difference value is calculated as $\delta_{ex/an} = 100 \cdot |(\sigma_{\omega,an} - \sigma_{\omega,ex}) / \sigma_{\omega,an}|$.

analyzed position			normal stress			difference
gauge	$x_{T,i}$ [mm]	$y_{T,i}$ [mm]	$\sigma_{\omega,ex}$ [MPa]	$\sigma_{\omega,an}$ [MPa]	$\sigma_{\omega,FEM}$ [MPa]	$\delta_{ex/an}$ [%]
T ₁ / T ₆	3	4	21.65	24.79	59.55	12.67
T ₂	11	4.5	15.67	16.62	27.07	5.72
T ₃	19	2.75	11.08	11.21	11.27	1.2
T ₄	794	-2.75	-9.64	-11.19	-19.21	13.87
T ₅	800	-2.5	-10.97	-13.76	-27.28	20.31

Table 3: Comparison of calculated and measured normal stresses in beam's longitudinal direction.

A more visual interpretation of the normal stress flow is depicted in Figure 11 showing significant differences between analytical and numerical (ANSYS) results. Experimental investigation has confirmed the proposed analytical and semi-analytical predictions well.

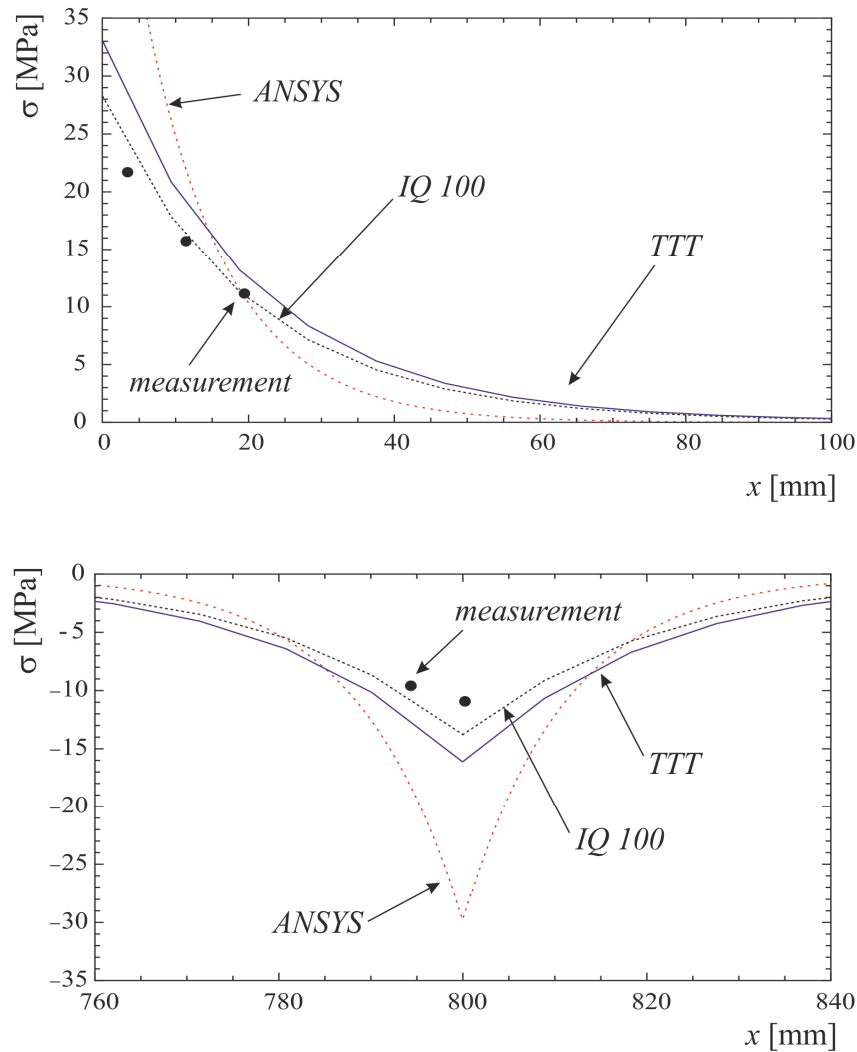


Figure 11: Normal stress distribution along the beam's longitudinal direction: measured values in comparison with numerical (ANSYS Beam188) and theoretical results re-calculated to gauges' positions.

The first four measurements are in very good agreement with the theory. However, there is an almost 2 MPa difference in the last measured value. Also, the total torsion angle measured is $\varphi = 3.25^\circ$ which gives a 25.23 % difference in comparison with theoretical result. Both discrepancies can be caused by imperfection in the external torque application which will be improved with device-modifications currently in process. The small values of warping displacement (see above) were immeasurable with the micro-displacement-meter.

5 Conclusions

This paper represents a valuable contribution in the analysis of thin-walled beams subject to non-uniform torsions. Authors' novel approach includes semi-analytical and numerical analyses and measurement of some key warping-torsion features such as normal (bimoment) stress flow, torsion angle and warping displacement for both open and closed cross-sections. For the measurement a specially designed measurement device has been built. The majority of the obtained results are in a good agreement with theoretical predictions. However, numerical analysis of the closed cross-sections, as carried out using commercial software [6], differs significantly from measurement.

As expected, the importance of the inclusion of warping in the analysis of both open and closed cross-sections has been confirmed experimentally. This is in contradiction with the widely used eurocodes [4], [5]. The measurements have also verified the necessity of the secondary torsion moment deformation effect consideration especially in closed cross-sections analyses.

In their future work, the authors will focus on a complex analysis of thin-walled structures that will include the Thin Tube Theory, Boundary Element Method and Finite Element Method using beam, shell and solid elements. In addition, the disproportion in calculations of the warping constant and secondary torsion constant will be analyzed and evaluated.

Acknowledgement:

This paper has been supported by Grant Agency VEGA (grant No. 1/0534/12).

References

- [1] V.Z. Vlasov, "Tenkostěnné pružné průty", Praha, SNTL, 1962.
- [2] K. Roik, G. Sedlacek, "Theorie der Wölbkrafttorsion unter Berücksichtigung der sekundären Schubverformungen - Analogiebetrachtung zur Berechnung des querbelasteten Zugstabes", Stahlbau, 35, 43, 1966.
- [3] H. Rubin, "Wölbkrafttorsion von Durchlaufträgern mit konstantem Querschnitt unter Berücksichtigung sekundärer Schubverformung", Stahlbau, 74, Heft 11, 826, 2005.
- [4] EC-3 Eurocode 3. Design of steel structures.
- [5] EC-9 Eurocode 9. Design of aluminium structures.
- [6] ANSYS Swanson Analysis System, Inc., 201 Johnson Road, Houston, PA 15342/1300, USA.
- [7] RSTAB, Ingenieur - Software Dlubal GmbH, Tiefenbach, 2006.
- [8] E.J Sapountzakis, V.G. Mokos, "3-D beam element of composite cross-section including warping and shear deformation effect", Computers and Structures, 85, 102, 2007.

- [9] V.G. Mokos, E.J. Sapountzakis, “3-D beam element of variable composite cross-section including warping effect”, *Acta Mechanica*, 171 (3-4), 703, 2004.
- [10] H. Rubin, “Torsions-Querschnittswerte für rechteckige Hohlprofile nach EN 10210-2: 2006”, *Stahlbau*, 76, Heft 1, 2007.
- [11] H. Rubin, “Zur Wölbkrafttorsion geschlossener Querschnitte und ihrer Irrtümer - Grundlagen”, 29th Stahlbauseminar, Band 140, ISSN: 1615-4266, 2007.
- [12] H. Rubin, M. Aminbaghai, “Wölbkrafttorsion bei veränderlichen, offenem Querschnitt - hat die Biegezugstabanalogie noch Gültigkeit?”, *Stahlbau*, 76, 747, 2007.
- [13] H. Rubin, M. Aminbaghai, H. Weier, “IQ-100. The civil engineering structures program”, TU Vienna, Bautabellen für Ingenieure, Werner Verlag, 17. Auflage, 2006.
- [14] H. Rubin, “Baustatik 2, Manuskript der Vorlesung. Institute of Structural Analysis”, Vienna University of Technology, 2007.
- [15] J. Murin, V. Kutis, “An Effective Finite Element for Torsion of Constant Cross-Sections Including Warping with Secondary Torsion Moment Deformation Effect”, *Engineering Structures*, ISSN 0141-0296, Vol. 30, Iss. 10, 2716-2723, 2008.
- [16] V.G. Mokos, E.J. Sapountzakis, “Secondary torsional moment deformation effect by BEM”, *International Journal of Mechanical Science*. IJMS-10323R1. Accepted for publication, 2011.
- [17] V.G. Mokos, E.J. Sapountzakis, “A Three-Dimensional Beam including Torsional Warping and Shear Deformation Effects arising from Shear Forces and Secondary Torsional Moments”, in B.H.V. Topping, Y. Tsompanakis, (Editors), “Proceedings of the Thirteenth International Conference on Civil, Structural and Environmental Engineering Computing”, Civil-Comp Press, Stirlingshire, UK, Paper 137, 2011. doi:10.4203/ccp.96.137
- [18] J. Murin, T. Sedlar, A. Kalas, V. Kralovic, “A device for measurement of non-uniform torsion of the thin-walled cross-sections”, Patent 6017 Slovak Republic, 2012 (In Slovak).
- [19] H. Rubin, “Vorlesung: BAUSTATIK 2. Grundlegende Formeln der Theorie II. Ordnung”, Institut für Baustatik TU Wien, 2009.